Current Biology 19, 108–114, January 27, 2009 ©2009 Elsevier Ltd All rights reserved DOI 10.1016/j.cub.2008.11.061

Report

# A Novel Vertebrate Eye Using Both Refractive and Reflective Optics

**Hans-Joachim Wagner,[1] Ron H. Douglas,[2,*] Tamara M. Frank,[3] Nicholas W. Roberts,[4,6] and Julian C. Partridge[5]**

[1]Anatomisches Institut
Universität Tübingen
Österbergstrasse 3
72074 Tübingen
Germany

[2]Henry Welcome Laboratory for Vision Sciences
Department of Optometry and Visual Science
City University
Northampton Square
London EC1V 0HB
UK

[3]Center for Ocean Exploration and Deep-Sea Research
Harbor Branch Oceanographic Institute
Florida Atlantic University
5600 U.S. 1 N
Fort Pierce, FL 34946
USA

[4]The Photon Science Institute
School of Physics and Astronomy
University of Manchester
Manchester M13 9PL
UK

[5]School of Biological Sciences
University of Bristol
Woodland Road
Bristol BS8 1UG
UK

## Summary

**Sunlight is attenuated rapidly in the ocean, resulting in little visually useful light reaching deeper than ~1000 m in even the clearest water [1]. To maximize sensitivity to the relatively brighter downwelling sunlight, to view the silhouette of animals above them, and to increase the binocular overlap of their eyes, many mesopelagic animals have developed upward-pointing tubular eyes [2–4]. However, these sacrifice the ability to detect bioluminescent [5] and reflective objects in other directions. Thus, some mesopelagic fish with tubular eyes extend their visual fields laterally and/or ventrally by lensless ocular diverticula, which are thought to provide unfocused images, allowing only simple detection of objects, with little spatial resolution [2–4]. Here, we show that a medial mirror within the ventrally facing ocular diverticulum of the spookfish, *Dolichopteryx longipes*, consisting of a multilayer stack derived from a retinal tapetum, is used to reflect light onto a lateral retina. The reflective plates are not orientated parallel to the surface of the mirror. Instead, plate angles change progressively around the mirror, and computer modeling indicates that this provides a well-focused image. This is the first report of an ocular image being formed in a vertebrate eye by a mirror.**

*Correspondence: r.h.douglas@city.ac.uk
[6]Present address: Department of Biology, Queens University, Kingston, ON K7L 3N6, Canada

## Results and Discussion

The eyes of *Dolichopteryx longipes* have been described once before [6]. However, relying on a single formalin-fixed specimen, this study was understandably incomplete and, in places, erroneous. On a recent expedition, we caught a live specimen of this species, allowing a more thorough description of its eyes.

### General Ocular Morphology and Eyeshine

In dorsal view, *D. longipes* has two upward-pointing eyes, each with a dark swelling on its lateral face (Figures 1A and 1B). Histological sectioning shows that each eye consists of two parts, largely separated by a dividing septum: the main, cylindrical, "tubular" eye (approximately 6 mm high and 4 mm wide) and a smaller, ovoid outgrowth from the lateral wall of the cylinder (the diverticulum, approximately 2.6 mm maximum height and 2.2 mm maximum width) (Figure 2). Both parts are enclosed in a common scleral capsule, consisting of hyaline cartilage and dense fibrocollagenous tissue covered in part by an epithelial epidermis. A reflective argentea, serving to camouflage the eye, lies internal to these transparent outer tissues, giving most of the eye a silvery appearance (Figure 1D). Inside this, much of the eye is lined by a pigmented choroid and photosensory retina (Figure 2). Two transparent areas, consisting only of modified sclera and epithelial tissue, interrupt the silvered outer surface of the eye; the conventional cornea, covering the dorsal surface of the tubular eye (Figure 2), and a ventral "cornea" in the diverticulum (Figures 1D, 3A, and 3F). The argentea is also lacking on the dorsal surface of the diverticulum, which appears dark due to the melanin-containing choroid (presumably so the diverticulum, which protrudes from an otherwise slender body, will blend into the dark background when viewed from above) (Figure 1B).

Flash photography of the dorsal and ventral surfaces of the live fish produce eyeshine in the main tubular eyes (Figure 1B) and the diverticula (Figure 1C), respectively, confirming their respective upward and downward gazes. Since the rod outer segments are separated from the argentea by a continuous layer of melanin-containing retinal pigment epithelial (RPE) cells and the pigmented choroid, the argentea cannot be responsible for the eyeshine. Instead, it is due to a tapetum located in the vitread parts of the RPE cells. In the case of the main tubular eye, the eyeshine is reflected directly from this tapetum. Within the diverticulum, however, light cannot reach the retina directly through the ventral cornea and is reflected onto the photosensory surfaces by a mirror on the dorsomedial wall of the diverticulum (Figure 2), whose reflective nature is most easily seen in dark-field illumination (Figure 3A).

### Morphology of the Diverticulum

Retinal tissue in the diverticulum is restricted to the lateral, caudal, and rostral surfaces, whereas the medial wall, which

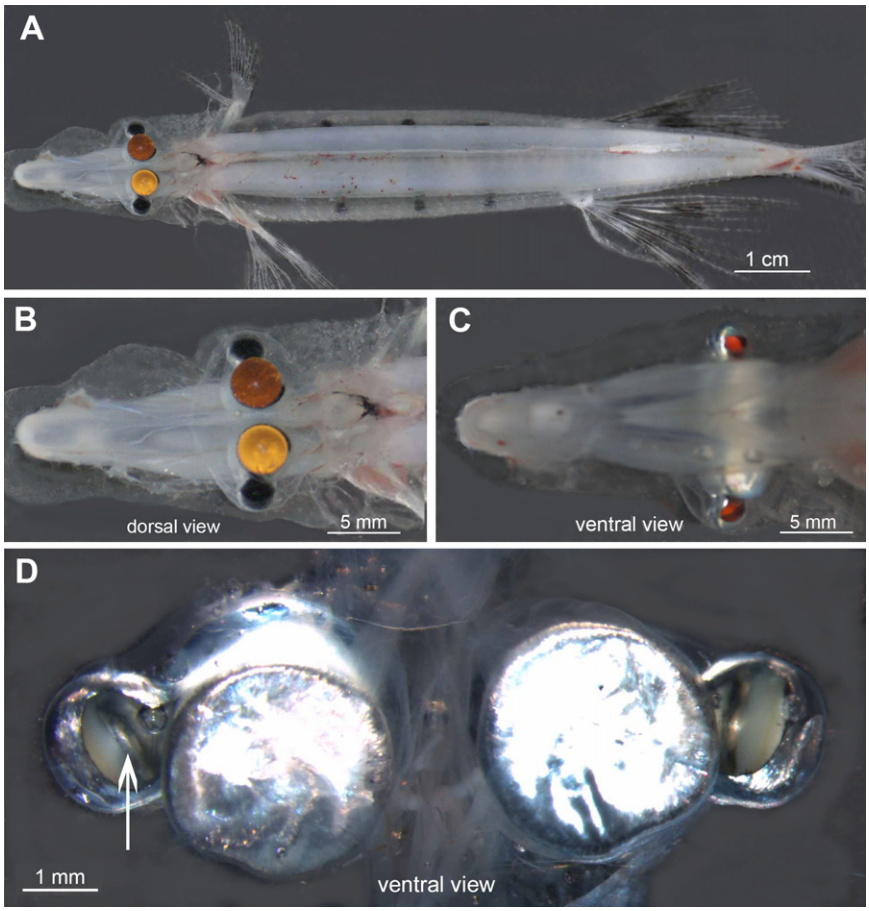


Figure 1. Surface Morphology of *Dolichopteryx longipes*

(A–C) Flash photographs of a recently captured *D. longipes* in both dorsal (A and B) and ventral (C) view. Note the yellow-orange eyeshine in the main tubular eyes in the dorsal view and the eyeshine from the diverticulum when viewed ventrally. The black structures lateral of the main eyes in the dorsal view are the upper surfaces of the diverticula.

(D) Ventral view of both eyes removed from the head, showing the silvery argentea on the base of the main eye. The ventral edge of a "mirror" within the diverticulum (arrow) is clearly visible through a transparent ventral "cornea."

forms the septum between the main eye and the diverticulum, is covered by a reflective layer more than 200 μm thick, composed of stacks of plates and occasional flat nuclei (Figures 2 and 3A–3C). As a result of mechanical stress during sectioning, some of the crystals within the plates have been dislocated, but in general they are arranged in approximately parallel stacks and have distinctly different orientations in different parts of this mirror (see below).

The retina within the diverticulum is broadly similar to that in the main retina and shows considerable regional variations (Figures 2 and 3A). Peripherally, it is simple and thin, with the thickness increasing more than 5-fold toward the center of the lateral wall. Rod outer segments in the periphery form a single layer and are about 40 μm long, whereas in the center, the photoreceptor layer is about 300 μm thick, with five to eight layers of rod inner and outer segments.

In sections taken near the center of the diverticulum (Figure 2), the retinae in the diverticulum and main tubular eye appear separate. However, serial sectioning and reconstruction (not shown) demonstrates that in more rostral and caudal sections, the retinae of the two parts of the eye are in fact continuous. In Figure 2, the ventral continuity between retinae of the diverticulum and the main eye is apparently broken by the diverticular cornea. In reality, the continuity is preserved because at its ventral edge, the diverticular retina thins abruptly, and the resulting two-layered epithelium bends sharply dorsally, covering the inner face of the diverticular retina (Figures 3A and 3E). Dorsally within the diverticulum, this epithelium is closely apposed for a short distance to an outer sheet of similar ciliary epithelium (originating dorsally from the main tubular eye and laterally forming the diverticular retina) but then transforms into the mirror forming the medial wall of the diverticulum. The layer that is derived from the RPE forms the reflective material, and the layer originating from the neural retina differentiates into a thin sheet of melanosome-containing epithelium facing the tubular eye. Thus, the "mirror" in the medial wall of the diverticulum is not homologous with the argentea but is a form of retinal tapetum.

### Optics of the Diverticulum

Both bright- and dark-field images (Figure 2 and Figures 3A–3C) of the diverticulum mirror show that it contains well-ordered crystals of high refractive index. As in the argentea, ocular tapeta, and scales of other fish [7–9], these are probably guanine plates.

Measurements from a contrast-enhanced light-microscopic transverse section showed that plate angles, measured at the lateral surface of the mirror, changed progressively from the ventral to the dorsal parts of the mirror (Figure 4A). When indexed by the angle (x) from the geometric center (shown in Figure 4C) of the mirror's lateral surface, a linear increase in plate angle (y) was apparent for values of x between −0.4 and 1.1 radians (or −22.9° and 63.0°). Linear-regression analysis showed that the slope of the regression line was highly significantly greater than zero, indicating that plate angle increases as the angle from the geometric center increases (slope = 0.4136, 95% CI = 0.359080–0.468100, $t_{92} = 15.07$, $p < 0.001$, $y = 2.107 + 0.4136x$, $r^2 = 0.71$). At values of x between 1.1 and 1.3 radians (i.e., in the most dorsal part of the mirror), plate angles did not conform to this relationship and were treated as outliers (Figure 4A), given that they were most likely caused by artifactual deformation of the mirror during fixation and sectioning.

A Matlab model that traced rays to produce a well-focused image resulted in predictions of the relationship between reflective plate angle (y) and angle from the geometric center of the mirror (x). Regression analysis showed that the ideal theoretical relationship was highly significantly different from zero (slope = 0.4125, 95% CI = 0.4111–0.4139, $t_{74} = 649$, $p < 0.001$, $y = 2.1102 + 0.4125x$, $r^2 > 0.999$). Moreover, when compared to the experimental measurements of plate angles, neither the predicted slope nor the predicted intercept were

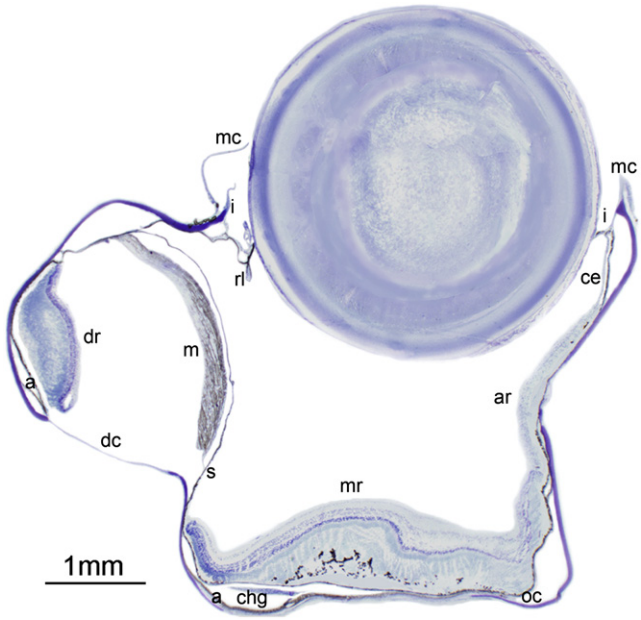


Figure 2. Transverse Section of the Entire Right Eye of *Dolichopteryx longipes*, Showing Both a Main, Upwardly Directed Tubular Portion and a Laterally Directed Diverticulum

The section was taken 522 μm from the rostral edge of the eye. Abbreviations are as follows: a, argentea; ar, accessory retina; ce, ciliary epithelium; chg, choroid gland; dc, diverticular cornea; dr, diverticular retina; I, iris; m, mirror; mc, main cornea (partially removed for facilitating the impregnation of tissue with resin); mr, main retina; oc, outer coats of the eye, consisting of sclera, argentea, and choroid; rl, *retractor lentis* muscle (ventral part); s, septum between the main tubular eye and the diverticulum.

significantly different from the corresponding observed values (intercept: estimate of the difference = 0.0028, 95% CI for difference = −0.0296–0.0239, $t_{93} = -0.21$, $p = 0.834$; slope: estimate of the difference = 0.0011, 95% CI for difference = −0.0534–0.0556, $t_{93} = 0.04$, $p = 0.968$), and predicted and observed linear regressions were virtually indistinguishable (Figure 4A).

To account for artifactual displacement of diverticular structures during tissue preparation (see Experimental Procedures), the model fitted the data observed for plate angles when the mirror was translated 0.19 mm toward the main tubular eye and 0.1 mm upwards to abut the dorsal cartilaginous scleral boundary of the diverticulum. The mathematical model was relatively insensitive to vertical displacements of the mirror. This is fortunate, because such displacements may have occurred in our histological sections, given that the mirror is clearly separated from the sclera by a void that is almost certainly an artifact. Moreover, movement of the mirror to a more medial position (i.e., toward the main tubular portion of the eye) may also have occurred, given that both diverticula and tubular eyes have suffered hydrostatic collapse as a result of dissection and the boundary between the two parts of the eye is not rigidly cartilaginous. The model predicts that the primary viewing angle of the diverticulum is 248°, measured as a polar angle [10] from the horizontal (Figure 4E).

With the modeled function used for plate orientation, rays traced from a distant point source located at the primary angle (248°; 68° below the horizontal) to the diverticulum were focused in the outer limiting membrane at the retina's vertical midpoint. At this point, the image is predicted to be optically sharpest (Figure 4E).

Ray tracing from distant point sources at angles offset from the primary axis of the diverticulum showed that the mirror provides a well-focused image over most of the retina (Figures 4C–4G). The diverticulum's predicted field of view in the lateral direction is from about 224° to about 272° (i.e., about 24° either side of the primary axis; 270° being directly downwards and 180° being lateral) (Figure 4B). For rays close to the vertical, only part of the mirror's surface is utilized, due to self-shading, and illuminated rods (i.e., those located toward the dorsal margin of the diverticular retina) are predicted to experience lower irradiance, with rays incident over a narrow range of angles, and therefore are potentially underfilled. The image brightness at such points will therefore be lower than for more lateral parts of the field of view. See Movie S1 for illustration of the results of the ray-tracing modeling.

Extensive comatic aberration (Figure 4H) results if the mirror is modeled as though it were "front silvered" (i.e., with the reflective crystals oriented parallel to the surface of the mirror; see Movie S2 for a computer simulation of ray tracing in such an eye). The orientation of reflective plates for such a mirror, being equal to the angle from the mirror's geometric center plus $\pi/2$ radians, is grossly different from that observed (as shown in Figure 4A).

We have concentrated on the potential imaging of distant sources and have not calculated the quality of the optical image for nearby objects. A dynamic change in ocular anatomy, however, would be required if the diverticulum were to focus close objects, because the mirror would have to be moved away from the retina. Such accommodative movements would be small unless light sources were very close: for example, to focus objects 100 mm distant, a mirror displacement of about 0.03 mm is needed from that required for focusing distant sources. The *retractor lentis* muscle of the main tubular portion of the eye is attached in places to the septum separating it from the diverticulum (though not apparent in Figure 2, it is indicated by serial sectioning through the whole eye). Because the mirror lies on this septum, this muscle might cause appropriate accommodative movements of the mirror.

## The Advantages of Ocular Mirrors and Their Presence in Invertebrates

Mirrors based on interference from layers of material of differing refractive index are common in animals [11, 12]. Within the eye, reflective tapeta behind the retina are known to increase sensitivity in many phyla, and in some invertebrates, such as the scallop *Pecten* and the ostracod *Gigantocypris*, image formation is mediated by such mirrors [13]. However, in the eyes of these animals, the reflective layer is behind the photoreceptors and light must first traverse the retinal layers before being imaged on the photoreceptors, which will degrade the optical focus and reduce image contrast. In *D. longipes*, the reflection takes place before the light reaches the retina. The eyes of this species are, therefore, in some ways more like the reflecting superposition compound eyes of decapod crustaceans [14], which also use preretinal mirrors for image formation.

The reflective-plate orientation and the shape of the front surface of the *Dolichopteryx* diverticular mirror provide a solution to the problem of imaging away from the optic axis of the mirror so that the photoreceptive retina does not interfere with the incoming light. Such solutions normally require either a secondary mirror for diverting the primary image out of the optical path (as used in Newtonian or Cassegrain reflecting telescopes [15]) or the use of off-axis "decentered"

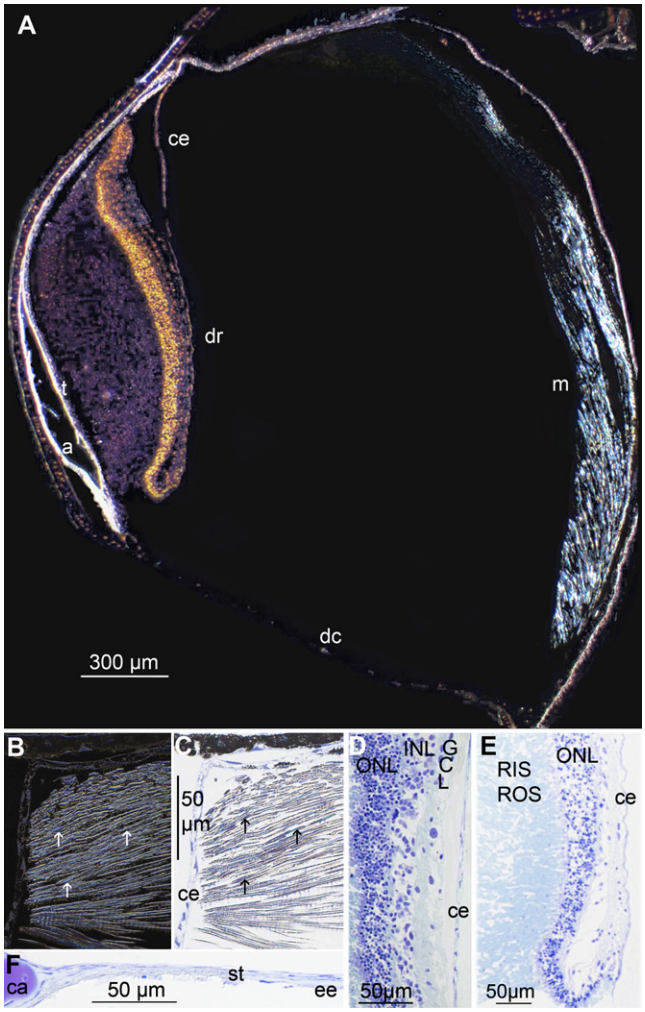


Figure 3. Detailed Morphology of the Ocular Diverticulum of *Dolichopteryx longipes*

(A) Transverse section of the entire diverticulum in dark field illumination, demonstrating the reflections of the mirror (m), the argentea (a), and the tapetum (t) of the diverticular retina (dr). As a result of the use of polarizing light and the specific orientation of the mirror's crystals, only the lower part of the crystals light up. Additional abbreviations are as follows: ce, ciliary epithelium (derived from the diverticular neural retina and the RPE), running medially over the retinal surface (which, dorsally, has become detached from the retinal surface); dc, diverticular cornea; oc, outer coats, consisting of sclera, argentea, and choroid.

(B and C) Dark field (B) and bright field (C) view of the dorsal edge of the mirror. The crystals within the plates of the multilayer stacks are highly refractive, resulting in artificial dark fringes in (C). The arrows indicate fusiform nuclei of the crystal-producing cells derived from the vitreal layer of the ciliary epithelium (ce). The pigment epithelium (PE) scleral to the mirror is continuous with the RPE of the diverticular retina.

(D) The inner layers (inner nuclear layer [INL] and ganglion cell layer [GCL]) of the diverticular retina contain fewer somata than the outer nuclear layer (ONL).

(E) At the ventral edge, the layers of diverticular retina narrow and transform into a ciliary epithelium, which doubles back on itself and covers the retina medially. Abbreviations are as follows: RIS, rod inner segments; ROS, rod outer segments.

(F) Lateral transition of the cartilagenous (ca) sclera and the cornea, composed of fibrocollagenous stroma (st) and a thin layer of epithelial epidermis (ee).

paraboloidal mirrors [16]. A priori, there is no reason that an "off axis" parabolic reflector could not have evolved in *Dolichopteryx*, and, indeed, the invertebrate ostracod *Gigantocypris* has a partially parabolic ocular mirror [12], though it is not used "off axis" and the retina is therefore in the optic path.

The use of a single mirror has a distinct advantage over a lens in its potential to produce bright, high-contrast images. Typically, vertebrate camera-type eyes (such as the tubular portion of the *Dolichopteryx* eye) are constrained to an *f*-number of approximately 1.25, in line with Matthiessen's principle [17]. Reflecting eyes, such as those of deep-sea crustaceans, can exhibit much greater collecting powers, with *f*-numbers considerably lower [18].

For reflecting systems such as the *Dolichopteryx* diverticulum, the *f*-number of a concave mirror is given by f/A, where f is the focal length of the mirror and A is the diameter of the entrance pupil. In the case of *Dolichopteryx,* the *f*-number of the mirror is 0.69. However, the unusual off-axis geometry of the diverticular mirror implies that the entrance-pupil diameter is not simply equivalent to the diameter of the mirror. Figure 4E illustrates how the entrance pupil is effectively about 1.39 mm for rays on the eye's primary axis (i.e., those focused to the retinal center). With a focal length of 1.63 mm (representing the distance from the central retina to the mirror surface), this corresponds to an effective *f*-number of approximately 1.17.

Therefore, compared to a normal fish's eye, the reflective optical system of the diverticulum achieves a greater light-gathering capability for extended sources. This, of course, requires photoreceptors to efficiently capture light arriving at angles of incidence outside their light-guiding acceptance angle, although this is typical of all vertebrate eyes. For point sources, such as distant bioluminescent flashes, however, entrance-pupil area rather than *f*-number is the appropriate anatomical measure of retinal illumination [17, 18]. In this case, use of the full mirror, rather than a smaller fraction of it (restricted by rods' light-guiding acceptance angle, here calculated to be 26.3° [19–21]), could potentially double photoreceptor light capture by rods at the central retina.

An increase of sensitivity in an eye often means a loss of spatial resolution, but to survive in the deep-sea, being able to see any light is nearly always of greatest benefit [17]. Although Figures 4C–4G suggest that aberrated peripheral rays may not be well focused by the mirror and therefore may reduce spatial resolution for some parts of the retina, an off-axis scheme still gains considerably in terms of resolution as compared to other mirror designs, because the light does not have to first pass through the retina.

As in the optically separated bilobed superposition eyes of many euphausiids and mysids and in the apposition eyes of hyperiid amphipods [13], the dorsally directed, lens-based, tubular portion of the *D. longipes* eye may function to silhouette dark objects against the residual sunlight, whereas the ventrally facing reflective diverticulum probably serves mainly to detect bioluminescent sources [22] (Figure 4B).

While invertebrates posses a plethora of eye designs, ranging from simple pinholes that focus light on the retina to simple and compound eyes based on single or multiple lenses or mirror optics, vertebrates appear to be more conservative, all eyes hitherto described utilizing a single lens to obtain a focused image. In this study, we have described an entirely novel image-forming vertebrate eye: one that forms an image by reflection. This demonstrates that image formation in vertebrates is not constrained to refraction, despite the evolutionary pathway taken, or retained, by most vertebrates.

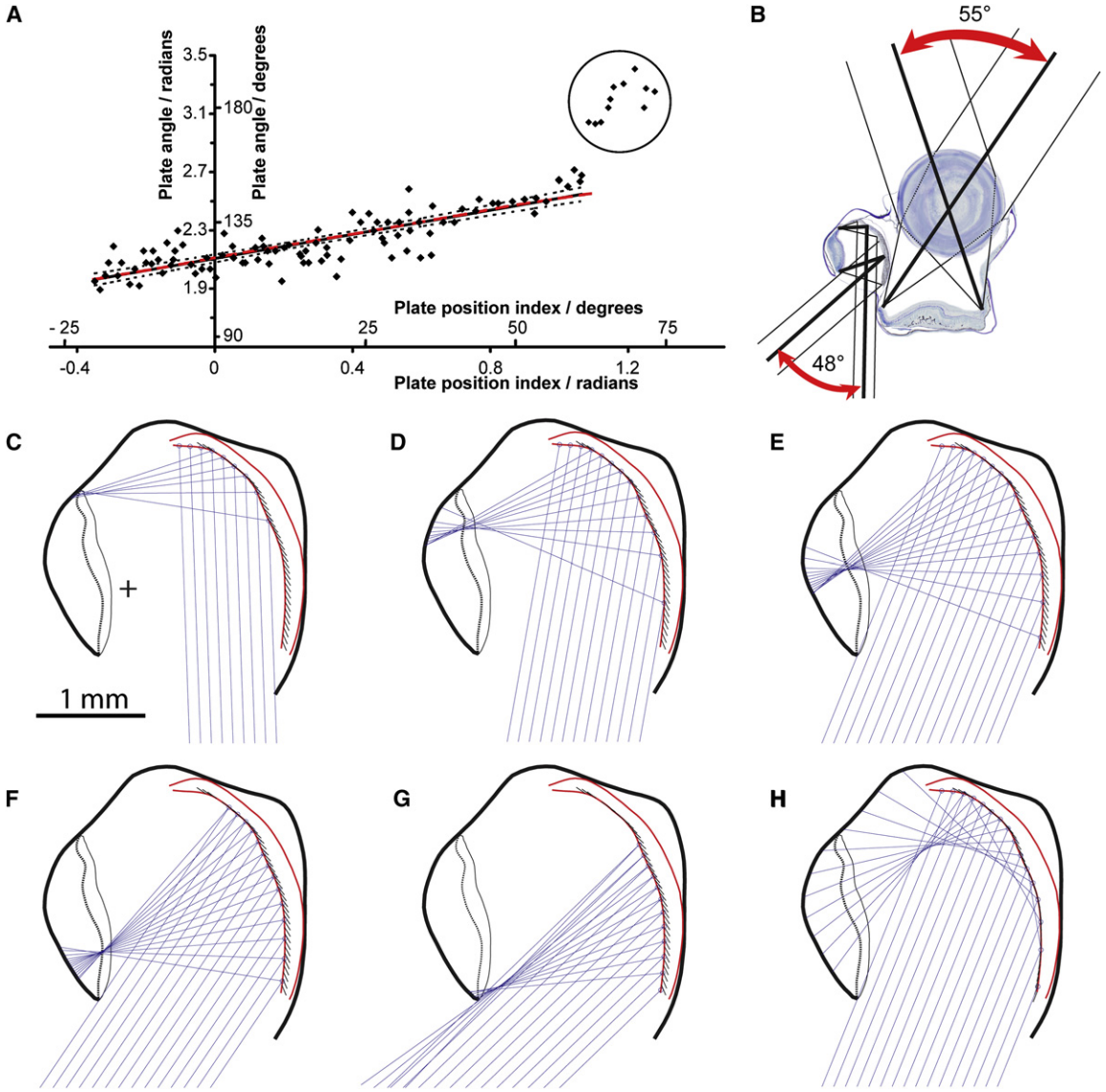


Figure 4. Optics of the Diverticulum

(A) Measured and predicted angles of reflective plates within the mirror of the ocular diverticulum. Plate position is indexed by an angle (x) from the geometric center (see Figure 4C) of the mirror's lateral margin to the plate position on the surface of the mirror. Plate angle (y) is the polar angle relative to the horizontal. The linear y on x regression line is shown (black line) with 95% confidence limits (dotted lines) for $x < 1.1$ radians ($x < 63^\circ$). It shows that plate angles are steeper toward the ventral part of the mirror and are closer to horizontal dorsally. Also shown is the regression line (red dashed line, almost entirely overlying the black line) through the points predicted by the Matlab model (see main text). Plates indexed by $x > 1.1$, located in the most dorsal part of the mirror, cannot be involved in image formation and were therefore treated as outliers (circled in figure).

(B) Frontal view of the right eye of *D. longipes*, showing the approximate fields of view of the dorsally directed tubular eyes and the ventrolaterally directed diverticulum.

(C–H) Schematic diagrams of a transverse section of the diverticulum, showing the output of a Matlab model that traced rays from distant point sources, located lateroventral to the diverticulum at various angles from the horizontal, to the retina. Incoming parallel rays of light are reflected from the mirror (the geometric center of which is marked "+" in Figure 4C) by reflective plates, which are shown as small black lines, oriented to show their predicted angles, behind the lateral (i.e., "front") surface of the mirror. Light reflected from the mirror is brought to a focus in the region of the retinal outer limiting membrane (indicated by the dotted line within the retina). Input ray angle is 272° in (C), 260° in (D), 248° (the primary viewing angle of the eye) in (E), 236° in (F), and 224° in (G). At input angles close to vertical, the mirror is underfilled, suggesting that retinal illumination will be lower toward its dorsal margin. Also shown (H) is the way in which the mirror would reflect light if the plate orientations were parallel with the surface of the mirror. The figure shows rays with an input angle of 248° and is thus directly comparable with Figure 4E. Such a "front silvered" mirror would be incompetent as an imaging device, because the focus would be well in front of the retina and subject to very high degrees of comatic aberration. In practice, such a mirror would also produce multiple reflections within the eye (not shown), further degrading the image.

## Experimental Procedures

### Animal

A single specimen of *Dolichopteryx longipes* (SL 102 mm) was caught with a Tucker trawl, with a 4 m × 3 m opening and fitted with a closing cod end, at 600–800 m depth in the South Pacific, over the southern end of the Tonga trench (24° 0.378S, 175° 30.24W), during a cruise aboard the *FS Sonne* (cruise SO194).

Because many mesopelagic animals are rarely caught, their taxonomy is often poorly described and their identification can be uncertain. Therefore,

we outline identification of our animal in detail. Its unique appearance placed it within the Opisthoproctidae, a family with six genera. The elongate body and the presence of more than a single row of vomerine teeth identified it as belonging to the genus *Dolichopteryx*, which contains eight valid species [23]. Five of these, like our animal, have tubular eyes (*D. pseudolongipes*, *D. longipes*, *D. anascopa*, *D. binocularis*, and *D. trunovi*). *D. pseudolongipes* and *D. trunovi*, unlike our specimen, have adipose fins. Several morphometric measures, including the distance between the snout and the origin of the pelvic fin, as well as the length of the pectoral fins as a proportion of the animal's standard length (70.5% and 17.6%, respectively), uniquely identify our animal as *D. longipes* rather than *D. anascopa* or *D. binocularis* [23] (Figure 1A).

### Photography

The animal was photographed immediately after capture from both the ventral and dorsal aspect, with a Sony Digital Single Lens Reflex A100 camera. The use of a Sony HVL-F36AM flash positioned close to the camera and aligned directly above or below the animal allowed the visualization of any eyeshine produced by light reflected from the ocular fundi of the tubular eye and diverticulum, respectively.

### Histology

The head of the animal was fixed in 4% formalin in seawater for 24 hr. After rinsing, it was transferred to 30% sucrose and, after equilibration, stored at −25°C. The complete right eye, with part of the upper head, was embedded in Epon and serially sectioned in the rostrocaudal direction (section thickness 2 μm) in the transverse plane and stained with methylene blue and Azur II [24].

### Optics of the Diverticulum

#### *Image Analysis*

For investigation of the optical performance of the diverticulum, digital images of a transverse section close to its midline were analyzed. Because tissues shrink during fixation, causing structures to separate along natural borders, the neural retina in histological sections of the diverticulum was separated from the choroid and RPE and displaced medially. It was assumed that the relatively rigid sclera was in its natural position. Consequently, prior to image analysis, TIFF color images were converted to monochrome, image contrast was increased, and the position of the retina was moved to the lateral scleral border with Adobe Photoshop. With the use of ImageJ image-analysis software [25], points delineating the outer sclera, the retinal vitreal surface, the retinal outer limiting membrane, and the lateral and medial surfaces of the mirror were digitized as Cartesian coordinates in calibrated SI units. The lateral surface of the mirror in the section was found to be a close approximation to a circle, and its geometric center was calculated (Figure 4C). This center point was thereafter used as an origin for an angular index to points on the surface of the mirror. The angles of the subcellular crystals within the mirror at these points were measured relative to the horizontal. All angles were referenced to standard Matlab polar coordinates.

#### *Modeling and Ray Tracing*

A Matlab (The MathWorks) computer program was written to predict the angles of the reflective plates within the diverticular mirror. These predictions were compared with the measurements of plate angles described above. This modeling "reverse engineered" the design of the mirror and the diverticulum and iterated certain variables of diverticulum anatomy (e.g., the position of the mirror relative to the diverticulum retinal outer limiting membrane, where rays were brought to a focus) to best fit the data for predicted and observed plate angles. The best estimate of the diverticulum's in vivo anatomy derived from this modeling allowed its likely optical performance to be ascertained in terms of image quality, image brightness, field of view, and angle of primary viewing direction.

In predicting reflective plate angles it was assumed that (1) rod outer-segment acceptance angles were 26.3° [19–21]; (2) all rod outer-segment longitudinal axes converged on a point medial to the mirror, such that all rod inner and outer segments make full use of potential reflections from the mirror (i.e., ideally, no rod inner and outer segments are "underfilled"); (3) the diverticulum has evolved to be optically best on its primary axis (i.e., the angle at which rays enter the diverticulum and are reflected to the central point of the outer limiting membrane); and (4) the mirror has been displaced horizontally and vertically from its in vivo position during tissue preparation. Finally, the modeling assumed that the diverticulum is looking at distant point (bioluminescent) sources of light.

### Supplemental Data

Supplemental Data include two movies and can be found with this article online at http://www.current-biology.com/supplemental/S0960-9822(08)01621-7.

### Acknowledgments

Thanks to the Master and crew of the *FS Sonne*. H.J.W. was funded by the Bundesministerium für Bildung und Forschung (03G0194A) and the Deutsche Forschungsgemeinschaft (Wa 348/24). R.H.D. was supported by a grant from the Royal Society. T.M.F. was funded in part by the National Science Foundation (IBN-0343871). N.W.R. was funded by the Engineering and Physical Sciences Research Council. We are grateful to Ulrich Mattheus for technical assistance and to Atsushi Fukui for help in species identification. We are also indebted to the four referees whose suggestions greatly improved this manuscript.

Received: September 22, 2008
Revised: November 17, 2008
Accepted: November 17, 2008
Published online: December 24, 2008

### References

1. Denton, E.J. (1990). Light and vision at depths greater than 200 meters. In Light and Life in the Sea, P.J. Herring, A.K. Campbell, M. Whitfield, and L. Maddox, eds. (Cambridge: Cambridge University Press), pp. 127–148.
2. Munk, O. (1966). Ocular anatomy of some deep-sea teleosts. Dana-Report *70*, 1–71.
3. Locket, N.A. (1977). Adaptations to the deep-sea environment. In Handbook of Sensory Physiology VIII/5; The Visual System of Vertebrates, F. Crescitelli, ed. (New York: Springer Verlag), pp. 67–192.
4. Collin, S.P., Hoskins, R.V., and Partridge, J.C. (1997). Tubular eyes of deep-sea fishes: A comparative study of retinal topography. Brain Behav. Evol. *50*, 335–357.
5. Widder, E.A. (1999). Bioluminescence. In Adaptive Mechanisms in the Ecology of Vision, S.N. Archer, M.B.A. Djamgoz, E.R. Loew, J.C. Partridge, and S. Vallerga, eds. (Dordrecht: Kluwer Academic Publishers), pp. 555–581.
6. Frederiksen, R.D. (1973). On the retinal diverticula in the tubular-eyed opisthoproctid deep-sea fishes *Macropinna microstoma* and *Dolichopteryx longipes*. Vidensk. Meddr. Dansk naturh. Foren. *136*, 233–244.
7. Ollivier, F.J., Samuelson, D.A., Brooks, D.E., Lewis, P.A., Kallberg, M.E., and Komaromy, A.M. (2004). Comparative morphology of the tapetum lucidum (among selective species). Vet. Ophthalmol. *7*, 11–22.
8. Denton, E.J. (1970). On the organization of reflecting surfaces in some marine animals. Philos. Trans. R. Soc. Lond. B Biol. Sci. *258*, 285–313.
9. Levy-Lior, A., Pokroy, B., Levavi-Sivan, B., Leiserowitz, L., Weiner, S., and Addadi, L. (2008). Biogenic guanine crystals from the skin of fish may be designed to enhance light reflectance. Cryst. Growth Des. *8*, 507–511.
10. Weisstein, E.W. "Polar Angle." From MathWorld–A Wolfram Web Resource. <http://mathworld.wolfram.com/PolarAngle.html>
11. Land, M.F. (1972). The physics and biology of animal reflectors. Prog. Biophys. Mol. Biol. *24*, 77–106.
12. Land, M.F. (2000). Eyes with mirror optics. J. Opt. Pure Appl. Opt. *2*, R44–R50.
13. Land, M.F., and Nilsson, D.-E. (2002). Animal Eyes (Oxford: Oxford University Press).
14. Vogt, K. (1980). Die Spiegeloptik des Flusskrebsauges. J. Comp. Physiol. [A] *135*, 1–19.
15. Hecht, E. (2002). Optics, Fourth Edition (San Francisco: Addison Wesley).
16. Howard, J.E. (1979). Imaging properties of off-axis parabolic mirrors. Appl. Opt. *18*, 2714–2722.
17. Warrant, E.J., and Locket, N.A. (2004). Vision in the deep sea. Biol. Rev. Camb. Philos. Soc. *79*, 671–712.
18. Land, M.F. (1980). Optics and vision in invertebrates. In Handbook of Sensory Physiology VII/6B, H. Autrum, ed. (Berlin: Springer Verlag), pp. 472–592.
19. Enoch, J.M. (1980). Vertebrate receptor optics and orientation. Doc. Ophthalmol. *48*, 373–388.

20. Snyder, A.W., and Pask, C. (1973). Stiles-Crawford effect - explanation and consequences. Vision Res. *13*, 1115–1137.
21. Enoch, J.M., Hudson, D.K., Lakshminarayanan, V., Scandrett, J., and Bernstein, M. (1990). Effect of bleaching on the width and index of refraction of goldfish rod and cone outer segment fragments. Optom. Vis. Sci. *67*, 600–605.
22. Land, M.F. (2000). On the functions of double eyes in midwater animals. Phil. Trans. R. Soc. B. *355*, 1147–1150.
23. Fukui, A., Kitagawa, Y., and Parin, N.V. (2008). *Dolichopteryx pseudolongipes*, a new species of spookfish (Argentinoidei: Opisthoproctidae) from the eastern Pacific Ocean. Ichthyol. Res. *55*, 267–273.
24. Richardson, K.C., Jarett, L., and Finke, E.H. (1960). Embedding in epoxy resins for ultrathin sectioning in electron microscopy. Stain Technol. *35*, 313–323.
25. Abramoff, M.D., Magelhaes, P.J., and Ram, S.J. (2004). Image Processing with ImageJ. Biophotonics International *11*, 36–42.